DOI: 10.1021/ma101743u

Macromolecules
ARTICLE

Glass Transition Behavior of PS Films on Grafted PS Substrates

Hoyeon Lee,[†] Hyungju Ahn,[†] Sudhakar Naidu,[†] Baek Seok Seong,[‡] and Du Yeol Ryu*,[†]

[†]*Department of Chemical and Biomolecular Engineering, Yonsei University, Seoul 120-749, Korea, and* [‡]*Korea Atomic Research Institute, Daejon 430-200, Korea*

David M. Trombly[§] and Venkat Ganesan*,[§]

[§]*Department of Chemical Engineering, University of Texas at Austin, Austin, Texas 78712, United States*

Received July 31, 2010; Revised Manuscript Received October 22, 2010

ABSTRACT: We present experimental results for the glass transition behavior of polystyrene (PS) films on grafted PS layers of the same chemical identity as a function of film thickness. Our results suggest that the T_g of PS films on brush substrates decreases with decreasing film thickness. The thickness dependence of T_g was observed to be more pronounced for the films on the shorter brushes with the high grafting density. We propose a qualitative rationalization of the observations by invoking both interfacial energy considerations as well as by adapting the percolation model for the glass transition of polymer films.

Introduction

The glass transition temperature is one of the key parameters determining the mechanical properties of polymers for different applications. Indeed, at the glass transition (with increasing temperature), the storage modulus (or melt viscosity) drops remarkably by a factor of thousands, while the volume and enthalpy begin to discernibly increase.[1] Not surprisingly, many prior studies have investigated a variety of phenomena and properties near the glass transition temperature of different polymeric materials.

More recently, research efforts have directed their efforts toward the impact of confinement, and specifically, the role of interfacial interactions upon the glass transition behavior of polymer materials.[2−8] Several experimental techniques have been used to probe this transition due to the changes in the volume and physical properties, including ellipsometry,[9−17] X-ray and neutron reflectometry,[18−25] atomic force microscopy,[26−28] Brillouin light scattering,[2,29] positron annihilation lifetime spectroscopy,[30−32] and fluorescence spectroscopy.[33−35]

Keddie et al. pioneered these researches where they observed a film thickness dependence of glass transition temperature (T_g) for polystyrene (PS) films on hydrogen-passivated Si wafers.[3] Compared to the T_g (∼100 °C) of the bulk material, a noticeable decrease in T_g was found as the film thickness (≤100 nm) was reduced. A similar but more significant decrease in T_g for freestanding PS films was observed by Forrest et al,[2,5] and Torkelson et al.[33−35] They suggested potentially two different mechanisms, arising from either the polymer chain confinement or a finite size effect depending on the characteristic molecular length scale. More insights into the influence of interfacial interactions were provided by the experiments of van Zanten et al., who observed an increase in T_g for poly(2-vinylpyridine) (P2VP) films on native oxide substrate of Si wafer with decreasing film thickness.[8] They attributed these trends to the fact that the substrate interactions are favorable with the polar P2VP. Furthermore, Keddie et al. demonstrated both an increase and decrease in T_g (with changing film thicknesses) can result for the same material by controlling the substrate interactions.[4] Explicitly, thin films of poly(methyl methacrylate) (PMMA) on a gold substrate that is unfavorable with PMMA displayed a decrease in T_g with decreasing film thickness, whereas for the films on native oxide substrate of Si wafer that is favorable with PMMA, they showed an increase in T_g with decreasing film thickness.

Many theoretical studies and computer simulations have also addressed the role of interfacial interactions upon the glass transition temperatures of polymer films[6,19,36] and have been discussed in a number of review articles.[37,38] Pertinent to the present study are the results by Torres et al. which indicated an increase or decrease in T_g (compared to the glass transition of the bulk) in ultrathin films strongly dependent on the strength of the interfacial interactions between the substrates and the polymer chains.[6,36] With decreasing film thickness, their results showed an increase in T_g for polymer films with the stronger surface energies, while a decrease in T_g was seen for polymer films with the weaker surface energy and for freestanding films. These results yet again have confirmed the importance of the interfacial interactions between the polymer chains and the substrate in influencing the confinement-induced glass transition behavior.

Grafting polymers to surfaces is commonly used as a means to tune the surface interactions with surrounding polymer matrices. Free polymer chains in contact with the grafted (or brush) polymer layer can show either wetting or dewetting (or segregation) behavior depending on the ratio of molecular weights of the matrix component to grafted polymer chains and the grafting densities of the brush component.[39−56] For polymer chains on the brushes of the same chemical identity, this behavior (termed "autophobic dewetting") can be attributed to the entropic effects of the matrix polymer and the grafted polymer chains.[40−44,47−56] More recently, we have investigated the dewetting behavior of a polymer matrix of different chemical identity on the brush substrates. Specifically, we studied the dewetting behavior of PMMA melts on grafted PS layers as a function of brush thickness (or grafting density),[57] and found, in agreement with theoretical calculations, that the behavior of this pair of chemically distinct melts was qualitatively similar to that expected for autophobic dewetting behavior.

*To whom correspondence should be addressed. E-mail: dyryu@yonsei.ac.kr; venkat@che.utexas.edu.

 Published on Web 11/10/2010

Table 1. Characteristics of PSOHs for the Surface Modification and PS in This Study

sample code	M_n	M_w/M_n	R_g[a] (nm)	grafting density[b] (σ; chains/nm^2)	brush thickness (d_0; nm)
PSOH-04	3700	1.08	1.666	0.688	4.0
PSOH-10	10000	1.05	2.739	0.554	8.8
PSOH-20	19500	1.05	3.824	0.379	11.7
PSOH-38	38000	1.09	5.339	0.210	12.6
PS (100K)	100000	1.02	8.660		

[a] Radius of gyration calculated by assuming linear PS chains. [b] Grafting density of underlying PS layers was evaluated by $\sigma = \rho d_0 N_A/M_n$, where ρ and N_A denote the mass density of PS (1.05 g/mol) and the Avogadro's number, and two variable parameters such as d_0 and M_n indicate brush thickness and the number-average molecular weight of PSOH, respectively.

In this study, we probe the inter-relationship between the interfacial interactions arising from grafted polymer layers and the T_g behavior of thin polymer films. This effort is motivated by two objectives: because grafting polymers is a common approach for dispersing particulate fillers in polymer matrices, it is of interest to know the manner in which the interfacial T_g properties of the polymer melt (i.e., the properties of the polymers matrix near grafted surface) differ from the bulk regions of the matrix. A second objective of this study is to probe whether interfacial energy considerations that have been used to explain the T_g behavior of thin polymer films near substrates can equally well be extended to rationalize the T_g behavior of thin polymer films on brush substrates.

We note that, in an earlier work by Tsui et al., a grafted random copolymer approach to surface modification was used to study the T_g behavior of PS films. In their study, the interfacial interactions on the substrate were controlled by the composition of random copolymers of styrene (S) and methyl methacrylate (MMA).[7] They presented intriguing results which are yet to be satisfactorily rationalized in terms of the interfacial energies. As another study pertinent to our work, Tate et al. considered the T_g of grafted PS polymers and noted a significant elevation in the T_g of brushes (relative to the bulk polymers) whose magnitude increased with increasing confinement.[58]

Our work presented in this article deals with conceptually more straightforward case of a polymer melt of the same chemical identity as that of the brush. With this model system, we investigate the glass transition behavior of PS films on a brush layer of the same chemical identity as a function of film thickness, where the brush thickness and grafting density of underlying PS layers are adjusted by the molecular weight of hydroxyl-terminated polystyrene (PSOH) that anchored onto the native oxide substrate of Si wafer. It was found that for the PS films the T_g decreases with decreasing film thickness of the polymer melt. Interestingly, the decrease in T_g turns out to be more significant for the films on the shorter brushes with higher grafting density. We provide a rationalization of the results by using mean-field theory to compute the melt-brush interfacial energy for the experimental parameters probed. Such considerations are also used in a percolation model for the glass transition to explain the observed thickness dependence.

A. Experimental Section

Polystyrene (PS) was synthesized by the living anionic polymerization of styrene in cyclohexane solution at 45 °C under purified argon using *sec*-butyllithium as an initiator. Number-average molecular weights (M_n) and polydispersity (M_w/M_n) of PS, characterized by size-exclusion chromatography (SEC) with multiangle laser light scattering (MALLS), were 100000 g/mol and 1.02, respectively. Four monodisperse hydroxyl-terminated polystyrenes (PSOH; purchased from Polymer Source, Inc.) were used to prepare grafted PS layers on the native oxide substrate of Si wafer, as listed in Table 1.

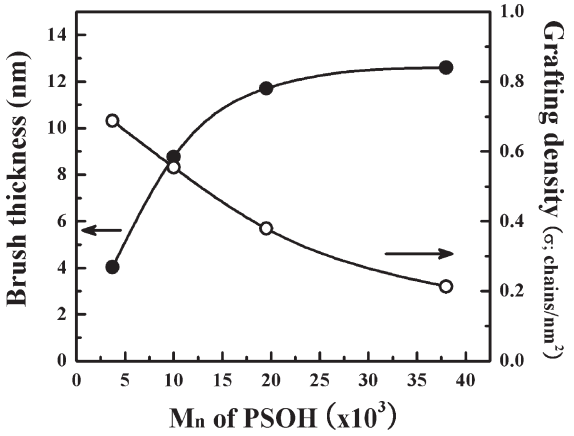

Figure 1. Brush thickness and the (calculated) grafting density (σ) for grafted PS layers as a function of the number-average molecular weight of PSOH.

The "grafting-to" surface modification was accomplished by spin-coating a film of PSOH from toluene solution then thermal annealing thin films at 170 °C under vacuum for 3 days. During annealing well above the glass transition temperatures (T_g) of PS (~100 °C), end-functional hydroxyl groups of PSOH diffuse and attach to the native oxide layer. After rinsing with toluene to completely remove the nonanchored chains, the thickness of the grafted PS layers was measured by ellipsometry.

The thickness of PS films was controlled from 30 to 140 nm on the grafted PS layers of various molecular weights of PSOH. After spin-coating, the PS films were annealed at 120 °C under vacuum for 12 h to remove the residual solvent in the films. This process produced the smooth surface topology of PS films within the surface roughness of 0.3 nm, which was observed by optical microscopy and scanning force microscopy (SFM ; Dimension 3100, Digital Instrument Co.) in tapping mode.

A heating chamber under vacuum was devised at the stage of a spectroscopic ellipsometry (SE MG-1000, Nanoview Co.), which is operated at an incidence angle of 70° with halogen light source of wavelength (λ) ranging from 350 to 850 nm (or 1.5−3.5 eV). Two ellipsometric angles (Ψ and δ) related to the film thickness were continuously monitored while heating the film samples at a constant rate of 2 °C/min. A thick film (300 nm) of crystalline polycaprolactone (PCL; 42500 g/mol) was used as a standard material for temperature calibration because it allowed a discernible melting temperature (~57 °C in the second run) in differential scanning calorimetry (DSC) even in the case of thin films. To obtain the precise spectroscopic changes in the sample films, we directly analyzed the temperature dependences of Ψ and δ at constant λ (553−563 nm) as a reference rather than thickness.

B. Results

Figure 1 shows the characteristic brush thickness and grafting density (σ) for grafted PS layers as a function of the number-average molecular weight (M_n) of PSOH, as presented in Table 1. Grafting density of underlying PS layers was evaluated by σ (chains/nm^2) = $\rho d_0 N_A/M_n$, where ρ and N_A denote the mass density of PS (1.05 g/mol) and Avogadro's number, and the parameters d_0 and M_n represent the brush thickness and the number-average molecular weight of PSOH, respectively. It can be seen that the low molecular weight PSOH-04 (3700 g/mol) has a brush thickness of 4.0 nm, at which PS chains are grafted densely at the substrate (0.688 chains/nm^2). With increasing molecular weight of PSOH, the brush thickness is measured to increase to 12.6 nm for PSOH-38 (38000 g/mol), while the grafting density decreases to 0.210 chains/nm^2, the latter decrease

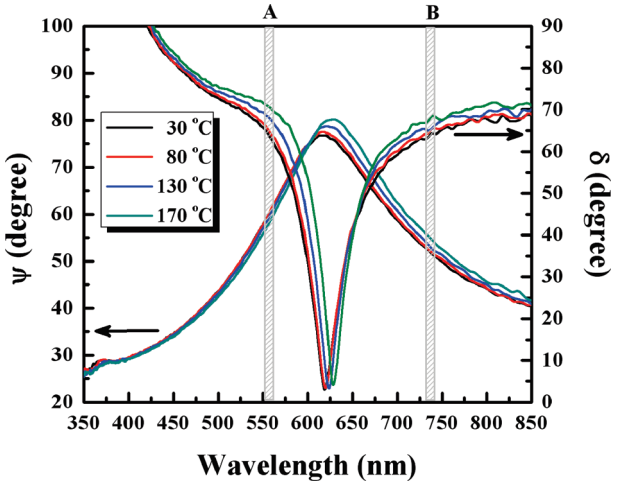

Figure 2. Ellipsometric angles of Ψ and δ for the PS film of 110 nm on a grafted PS layer prepared with PSOH-10 as a function of wavelength in a range 350 to 850 nm, which were measured at 30, 80, 130, and 170 °C. Two wavelength zones are indicated by A (553−563 nm) and B (734−744 nm).

is likely due to the low concentrations of the end-hydroxyl group and the slow diffusion of high molecular weight PSOH-38.

PS homopolymer of 100000 g/mol was spin-coated on grafted PS substrates and was followed by thermally annealing the PS films at 120 °C under vacuum for 12 h to remove residual solvent and to equilibrate thin films at interfaces. To reasonably evaluate the glass transition in polymer films, we first demonstrate the temperature dependence of ellipsometric parameters and data resolution. Figure 2 presents the changes in ellipsometric angles such as Ψ and δ for the PS film of 110 nm on a grafted PS layer prepared with PSOH-10, as a function of wavelength in a range 350 to 850 nm depending on the temperature measured. We selected two wavelength zones of 553−563 nm (indicated by A) and 734−744 nm (B) to avoid less temperature dependence at lower wavelength and the noise perturbation at higher wavelength, respectively. As temperature elevates from 30 to 170 °C, the values of Ψ decrease at A zone but increase at B zone due to a curve shift toward higher wavelength, while the values of δ increase at both zones. This temperature dependence on ellipsometric angles at two selected zone of wavelength ranges enable us to evaluate the glass transition in polymer films. It should be mentioned that ellipsometric angles are significantly influenced by the film thickness because decreasing film thickness drifts the curve toward lower wavelength.

Figure 3a and b show ellipsometric angles for the PS film of 110 nm on a grafted PS layer prepared with PSOH-10 as a function of temperature, which were analyzed at two wavelength zones of A and B, as described in Figure 2. At 102 °C, the identical value of Ψ at A zone begins to decrease remarkably, and the value of Ψ at B zone also begins to increase. A similar trend is seen in the values of δ with temperature, as shown in Figure 3b, leading to the identification of the glass transition temperature (T_g) for the film, determined by the intersection of the two linear regressions of glassy and rubbery temperature ranges in PS film. The changes of the slopes in ellipsometric angles, observed at a temperature (102 °C), prove that the glass transition is independent of wavelength we selected in ellipsometry. This behavior consistent with the T_g of the film is seen in the change of the film thickness displayed in Figure 3c, which is caused by the difference in the thermal expansion between glassy and rubbery states of amorphous polymers. For better characterization, we hereafter will consider the value of Ψ rather than δ to evaluate the T_g of thin films, because the changes in the slopes for the values of Ψ

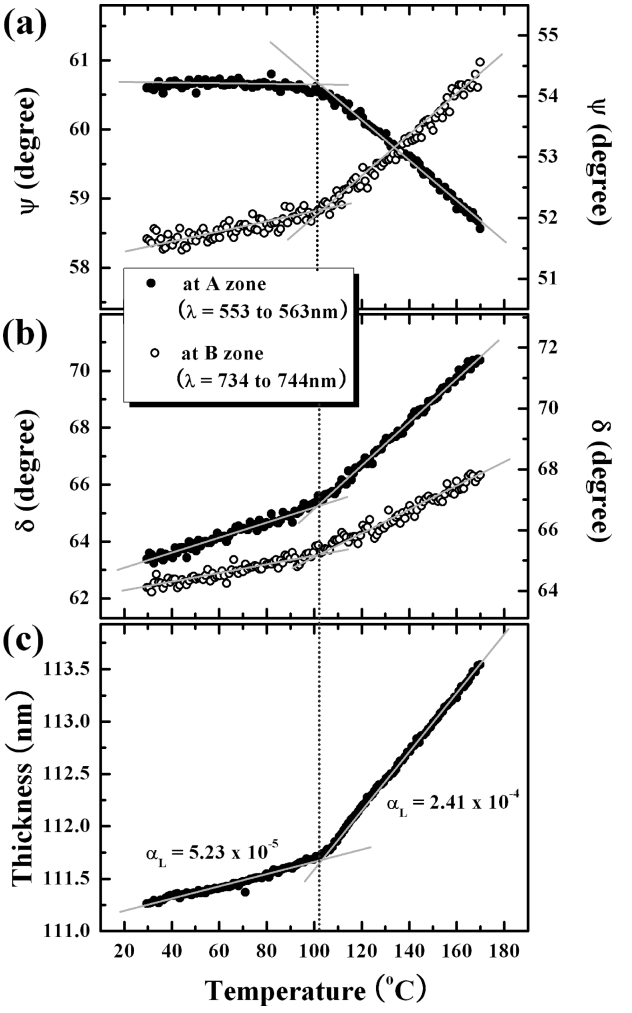

Figure 3. Ellipsometric angles of Ψ (a) and δ (b) for the PS film of 110 nm on a grafted PS layer prepared with PSOH-10 as a function of temperature, which were analyzed at two wavelength zones of (553−563 nm) and B (734−744 nm). (c) The corresponding film thickness evaluated by both ellipsometric angles and refractive index of the film. The dotted line indicates a consistent T_g at 102 °C for the film.

(especially at A zone) are more discernible than those for the value of δ.

Figure 4 shows the temperature dependence of the ellipsometric angle Ψ at a wavelength zone of A for the PS films of different thicknesses on a grafted PS layer prepared with PSOH-04. The T_g of the PS film of 110 nm was observed at 101 °C. It corresponds to the point of a rapid decrease for the value of Ψ because a wavelength zone of A for the film of 110 nm is placed at the left side of the maximum Ψ. In contrast, placing at the right side of the maximum Ψ produces a rapid increase for the values of Ψ with temperature, as are the cases for the other PS films of 70, 50, and 30 nm. With decreasing film thickness to 30 nm, T_g is seen to decrease to 81 °C. Such measurements were repeated for the different grafted PS layers, film thicknesses, and temperatures.

Figure 5 summarizes our results for T_g of the PS films on the various grafted PS layers as a function of film thickness. For a fixed grafted PS layer (or PSOH), a decrease in T_g of PS films is seen with decreasing film thickness. However, the variations with thickness are seen to be more significant for films on the shorter brushes with the higher grafting densities. Indeed, the *confinement effects* upon the T_g are seen to follow the sequence in this experiment: PSOH-04 > PSOH-10 > PSOH-20 > PSOH-38. The T_gs of thick PS films like 140 nm are constant (103 °C) and close

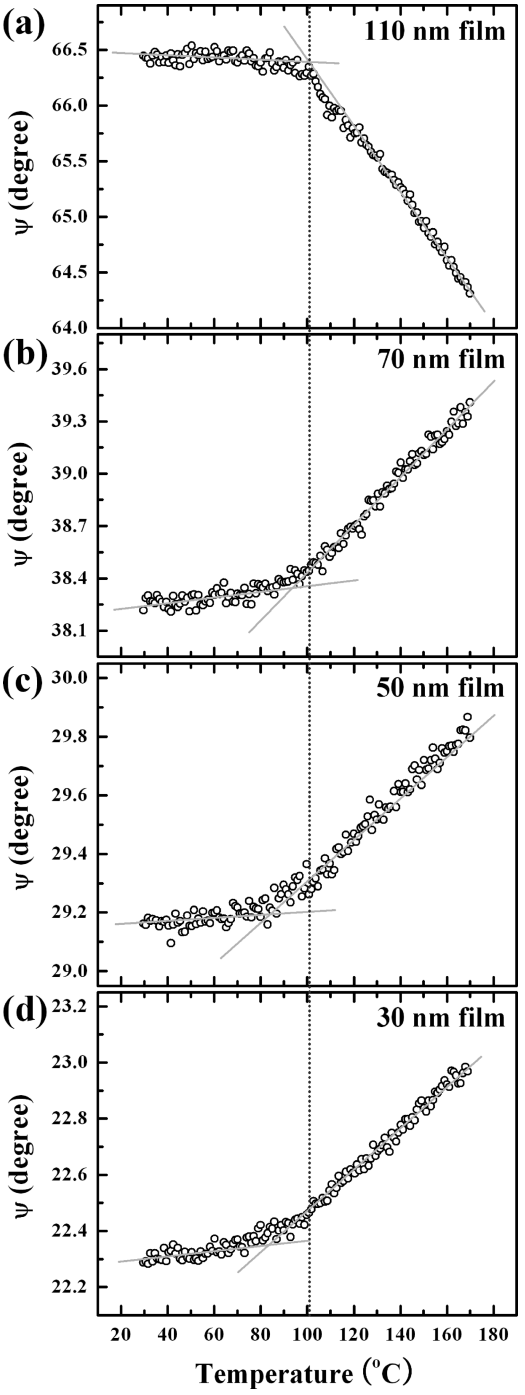

Figure 4. Ellipsometric angles of Ψ at a wavelength zone of A (553−563 nm) for the PS films on a grafted PS layer prepared with PSOH-04 as a function of temperature. Each film thickness of PS films is indicated. The dotted line indicates a T_g (101 °C) for the PS film of 110 nm to guide eyes.

to that (102 °C) of the bulk regardless of the brush thickness (or grafting density of underlying PS layers). In the next section, we provide a qualitative rationalization of the experimental observations.

C. Discussion

We note that there is still a lack of complete understanding of the origins of the T_g behavior of thin polymer films. A number of (not necessarily mutually exclusive) candidate explanations have been proposed, including effects such as density and/or free volume perturbations[19,59] arising from interfacial interactions, polymer mobility perturbations resulting from confinement and/or interfacial interactions,[38,60] confinement-induced changes in the energy landscape, and so on.[36] Below, we draw upon these earlier advances and propose two speculative hypotheses for rationalizing the experimental observations.

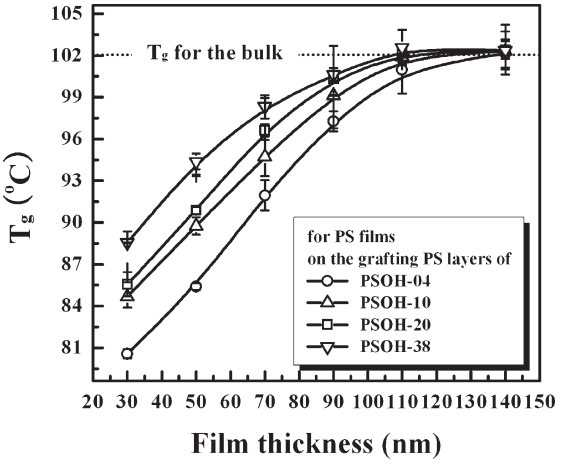

Figure 5. T_g as a function of film thickness for PS films on the various grafted PS layers (or PSOHs).

Our first hypothesis relies on considerations of interfacial energies. Despite the lack of consensus on the mechanistic underpinnings of T_g of thin films, it is generally accepted that on surfaces with which the polymer exhibits favorable interactions, the T_g of thin films tends to be enhanced with respect to bulk and increases further with confinement.[6,19,37,38] In contrast, for situations where the polymer is repelled by the substrate, the T_g of thin films tends to be lowered with respect to the bulk and decreases upon confinement. Keeping in mind that in the present study grafted PS layers screen the interactions from the native oxide layer of Si substrate, the mechanism responsible for the decrease in T_g with decreasing film thickness for the PS films is likely distinct from that arising due to the unfavorable interactions between the polymer and the bare substrate. Instead, the interfacial interactions between the polymer matrix and the brush is likely responsible for the experimental results in this study.

To verify the above hypothesis, we characterize the polymer brush-matrix (or melt) interfacial interactions by an "effective" interfacial tension parameter γ_{b-m} (the term "effective" is used to emphasize that the interfacial tension is not between two bulk phases). Prior researchers have used scaling theories,[61] strong segregation approximation,[57,62] and polymer self-consistent field theories[47,50] (SCFT) to quantify γ_{b-m} between a polymer brush and melt of the same chemical identity. Explicitly, γ_{b-m} has been computed as a function of the ratios of the molecular weights of the brush to matrix polymers and grafting densities of the brush. Such calculations have been used to shed light on the wetting−dewetting transitions of the matrix polymer. In the present work, we adapted the SCFT calculation methodology proposed by Matsen and Gardner[50] to calculate the interfacial tension γ_{b-m} for the experimental parameters. Because the accompanying theory and calculation procedures are very similar to that detailed in the article by Matsen and Gardner, we eschew repeating the details here. Shown in Figure 6 are the so-calculated γ_{b-m} for the four different polymer brushes considered in this study. The cases PSOH-04, PSOH-10, and PSOH-20 correspond to the dewetting situation, while PSOH-38 corresponds to a partially wetting situation (in this case the interfacial tension was obtained based on the free energy per unit area difference between an infinitely thick film and the coexisting polymer film of finite thickness).[50] It is evident that the interfacial tensions

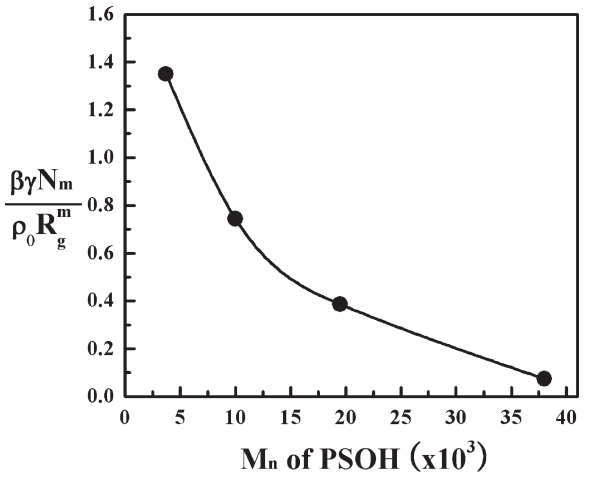

Figure 6. Brush−melt interfacial tension γ (normalized by $\beta=(k_BT)^{-1}$, number of segments in the polymer melt N_m, the molecular volume of segments ρ_0, and the radius of gyration of the melt polymers R_g^m) as a function of molecular weight of grafted PS brushes (or PSOHs) considered in this study.

follow the sequence γ_{b-m} (PSOH-04) > γ_{b-m} (PSOH-10) > γ_{b-m} (PSOH-20) > γ_{b-m} (PSOH-38). This result can be explained physically in terms of the lower stretching free energy incurred by longer brush chains to accommodate the interpenetration with the matrix chains. Because a larger interfacial tension correlates to stronger *unfavorable* interaction, the preceding results qualitatively rationalize the trends seen in the experimental observations in Figure 5.

An alternative, albeit more tentative, quantitative explanation for the shape of the curves in the experimental observations can be proposed based on dynamical considerations relating to the interpenetration between the polymer melt and the brush. To provide a physical picture of this hypothesis, we note that in the extreme situation of very high grafting densities and small molecular weights of the brush polymers, the melt chains have very little interpenetration with the brush chains. In such a case, the brush surface may be viewed as a "hard" repelling surface, and the matrix polymer mobilities near the brush surface may be expected to be enhanced relative to the bulk unperturbed state. Upon increasing molecular weights of the brush polymer, there is a thickening of the interpenetration zone between the matrix and the brush polymer. This result is quantitatively demonstrated in Figure 7a, which displays the interpenetration widths deduced from the SCFT volume fraction profiles for the melt and brush chains for the experimental parameters. The enhanced penetration between the matrix polymer and the brush is expected to increase the friction on the matrix chains and lead to a retardation of the dynamics of the matrix chains near the brush−melt interface relative to the case of no or little interpenetration. In an earlier work, a quantitative demonstration of such retardation effects was provided in the context of *melt dynamics* of block copolymer compatibilizers at polymer blend interfaces.[63−65] The results of the preceding work suggested that the length scale over which the retardation of dynamics persists correlates with the extent of brush−melt interpenetration, whereas the strength of such retardation effects were shown to correlate with the grafting density of the brush (expressed in units of squared radius of gyration of the brush chains, also shown in Figure 7a). An alternative physical picture that leads to a similar hypothesis is suggested by the experimental results of Tate et al.[58] in which the authors demonstrate a significantly elevated T_g for a film of grafted polymers. The latter results also indicate that the melt polymers in the interpenetration zone are in an environment of significantly reduced mobilities. Below, we adapt a simple phenomenological

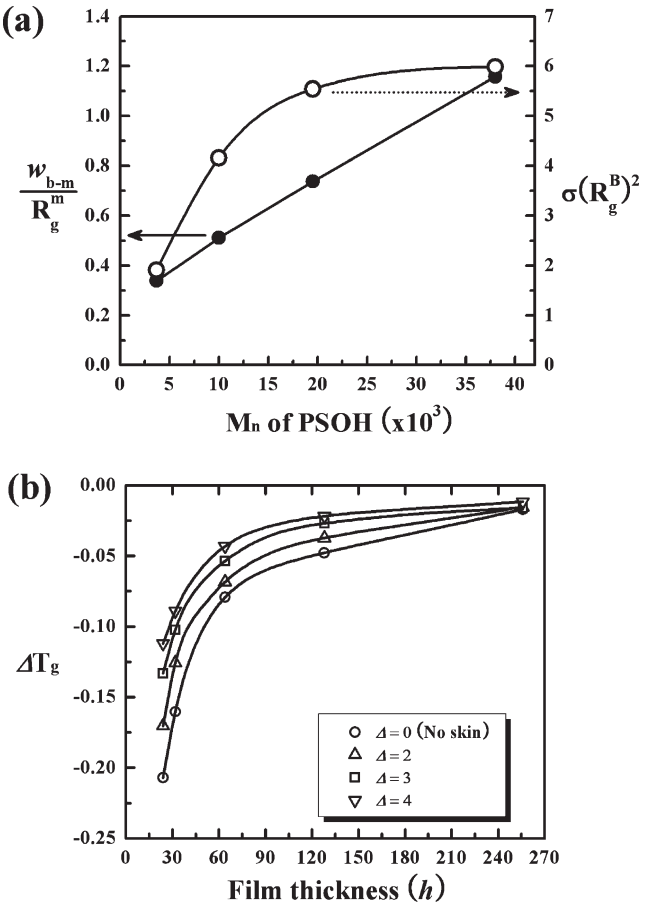

Figure 7. (a) Brush−melt interpenetration thickness w_{b-m} (normalized by R_g^m) and the grafting densities (expressed in units of $(R_g^B)^2$) as a function of molecular weight of grafted PS brushes (or PSOHs) considered in this study, and (b) Percolation model results for ΔT_g (defined as $T_g(h) - T_g(h=\infty)$, expressed in arbitrary units) as a function of film thickness (expressed in lattice units) for different skin thicknesses denoted by Δ.

model for glass transition to demonstrate the manner in which such dynamical retardation effects can rationalize the experimental results.

To provide a schematic illustration of the impact of the above effects on the T_g of thin polymer films, a static percolation model of glass transition was adapted,[66] which was previously used to model phenomena in thin films and polymer nanocomposites.[65,66] Such percolation models are based on the hypothesis that glass transition in materials occur as a result of the percolation of slow, immobile domains through the system. In a recent work,[66] Long and Lequex used such an idea in conjunction with bounding surfaces that accelerate and decelerate the dynamics to successfully explain the thickness dependence and the long-range nature of T_g changes in thin polymer films. While more recent work has cast doubts on whether such percolation models can suffice quantitatively to explain the phenomena,[67] nevertheless, we use it here for an illustration of the manner in which the above-discussed effects can lead to trends which qualitatively mirror the experiments. For this purpose, we follow our recent work[65,66] and incorporate the above surface interaction effects in such percolation models by including a "skin" of influence around the surface in consideration. Physically, such a skin represents the zone over which the polymer (matrix) dynamics is affected by the surface. Such a skin is characterized by two parameters, namely, the strength of influence and its thicknesses. Based on our discussion in the preceding paragraph, it is evident that in transitioning from shorter brushes to longer brushes, both these parameters are

enhanced. However, in the purely schematic spirit of this discussion, we just consider the influence of increasing the zone of influence of the substrate while keeping its strength a constant (allowing the strength of interaction to vary would only serve to enhance the effects reported below). The Appendix presents more details on the manner in which the percolation model is implemented, while the outcome of such analysis is depicted in the results displayed in Figure 7b. It is seen that the dynamical retardation effects tend to enhance the T_g relative to the unperturbed case. Such effects are seen to become more pronounced as the thickness (of the polymer film) is reduced and approach the bulk T_g for large thicknesses. More importantly, larger skin zones of influence are seen to lead to more significant effects. Taken in conjunction with the results presented in Figure 7a (which quantifies the "skin thickness" as a function of the brush molecular weights), the result of Figure 7b rationalizes the experimental result of Figure 5 and provides a qualitative picture which is strikingly similar to the trends noted therein.

D. Summary

In summary, in this work we presented an experimental investigation of the T_g of polymer films on grafted substrates of the same chemical identity. Our objective was to shed light on the influence of the different physical parameters upon the overall confinement-dependent T_g of polymer films. These results indicated that the T_g of the polymer films on such substrates were lowered relative to the bulk. More interestingly, the confinement effects were seen to become diminished with increasing molecular weight (and brush thickness) of grafted PS layers. These trends were rationalized by invoking two possible explanations. The first explanation relied on the interfacial free energies at the interface of brush and melt and its variations with increasing brush thickness of grafted PS layers. The second explanation relied on the dynamical effects which may arise in the overlap zone between the brush and melt polymers. It is likely that the experimental trends are a result of a combination of the preceding effects.

Our results suggest that brush substrates may serve as a facile means to tune the confinement effects upon T_g (and aging) of polymer films. Indeed, a variety of physicochemical interactions can be achieved by changing the grafting densities, molecular weights and the chemical identities of the brush polymers.[51] In addition to the practical importance, such studies may provide valuable insights which may allow one to sort through the different mechanisms speculated to be responsible for the confinement effects on the glass transition of polymer films.

Acknowledgment. This work was supported by the Nuclear R&D, APCPI ERC (R11-2007-050-00000), Midcareer Researcher Program (2010-0000052), and the Pioneer Research Center Program (2010-0019550) funded by the Ministry of Education, Science and Technology (MEST), Korea. V.G. acknowledges support from the National Science Foundation under Award Number 0730243, a grant from Robert A. Welch Foundation (Grant F1599), and the U.S. Army Research Office under Grant W911NF-07-1-0268. V.G. also acknowledge the Texas Advanced Computing Center (TACC) at The University of Texas at Austin for providing computing resources that have contributed to the research results reported within this paper. We thank Prof. Ophelia K. C. Tsui for helpful discussion and sharing of experimental data and Dr. Victor Pryamitsyn for useful discussions pertaining to the theoretical section of this article.

Appendix

In this section, we discuss the implementation of the percolation model used to generate the results of Figure 7b. Because much of the details are identical to those expounded in earlier publications,[66,68,69] we eschew repeating them here and instead refer the interested reader to the original references. Briefly, the percolation approach ascribes glass transition to a percolation of slow, immobile domains in the system. In a computational framework, this is accomplished by considering the *site* percolation transition on a lattice of the slow domains. The probability for occurrence of a slow domain is representative of the material characteristics and the temperature. The probability (temperature) at which there is a site percolation transition is ascribed as the glass transition temperature. Confined freely suspended films (repelling surfaces) are represented in this framework by considering the influence of bounding surfaces that possess lower probabilities for forming slow domains (representing the surface-induced enhancement in polymer mobilities). In such cases, the percolation of slow domains (in the direction parallel to the film) is expected to occur at a higher probability, representing a confinement-induced lowering of the T_g. Such a model was used by Long and Lequex[66] to explain the long-range nature of confinement-induced T_g effects (albeit, see Lipson and Milner[67] for some caveats regarding the quantitative nature of such effects).

In this work, we adapted the above model while incorporating interfacial zones near *one* of the confining surfaces (modeling the brush substrate). The other substrate was modeled similar to the case of freely suspended film. These interfacial zones were to be characterized by a length scale parameter Δ representing the thickness (in lattice units) of the interfacial zone. In addition, the skin zone was characterized by a parameter δ representing the (dynamical) strength of the interfacial interactions. Explicitly, the probability of forming a slow domain in the interfacial zones was assumed to be enhanced (relative to the bulk) by a factor $1 + \delta$. When this framework was used, the site percolation probability $p_c(h)$ for a *two-dimensional* lattice was determined as a function of the confinement thickness (in lattice units) h and the interfacial zone thickness Δ (as mentioned in the text, we chose to retain δ fixed at $\delta = 0.1$ in all the results). While the so-determined $p_c(h)$ can be related to the actual T_g pending knowledge of some phenomenological material parameters,[66] such an effort is unnecessary for the purely illustrative spirit in which we have used the percolation model. Whence, we ascribe $p_c(h = \infty) - p_c(h) = T_g(h) - T_g(h = \infty)$ up to an arbitrary prefactor. These results are displayed in Figure 7b.

References and Notes

(1) *Introduction to Physical Polymer Science*; Sperling, L. H. Ed.; John Wiley and Sons, Inc.: Hoboken, New Jersey, 2001.
(2) Forrest, J. A.; Dalnoki-Veress, K.; Stevens, J. R.; Dutcher, J. R. *Phys. Rev. Lett.* **1996**, *77*, 2002.
(3) Keddie, J. L.; J., R. A. L.; Cory, R. A. *Europhys. Lett.* **1994**, *27*, 59.
(4) Keddie, J. L.; J., R. A. L.; Cory, R. A. *Faraday Discuss.* **1994**, *98*, 219.
(5) Mattsson, J.; Forrest, J. A.; Börjesson, L. *Phys. Rev. E* **2000**, *62*, 5187.
(6) Torres; Nealey, P. F.; de Pablo, J. J. *Phys. Rev. Lett.* **2000**, *85* (15), 3221.
(7) Tsui, O. K. C.; Russell, T. P.; Hawker, C. J. *Macromolecules* **2001**, *34* (16), 5535–5539.
(8) van Zanten, J. H.; Wallace, W. E.; Wu, W.-l. *Phys. Rev. E* **1996**, *53*, R2053.
(9) Beaucage, G.; Composto, R.; Stein, R. S. *J. Polym. Sci., Part B: Polym. Phys.* **1993**, *31* (3), 319–326.
(10) DeMaggio, G. B.; Frieze, W. E.; Gidley, D. W.; Zhu, M.; Hristov, H. A.; Yee, A. F. *Phys. Rev. Lett.* **1997**, *78* (8), 1524–1527.
(11) Grohens, Y.; Brogly, M.; Labbe, C.; David, M.-O.; Schultz, J. *Langmuir* **1998**, *14* (11), 2929–2932.
(12) Kahle, O.; Wielsch, U.; Metzner, H.; Bauer, J.; Uhlig, C.; Zawatzki, C. *Thin Solid Films* **1998**, *313−314*, 803–807.
(13) Kawana, S.; Jones, R. A. L. *Phys. Rev. E* **2001**, *63*, 021501.

(14) Kim, J. H.; Jang, J.; Lee, D.-Y.; Zin, W.-C. *Macromolecules* **2001**, *35* (1), 311–313.
(15) Kim, J. H.; Jang, J.; Zin, W.-C. *Langmuir* **2000**, *16* (9), 4064–4067.
(16) Kim, J. H.; Jang, J.; Zin, W.-C. *Langmuir* **2001**, *17* (9), 2703–2710.
(17) Singh, L.; Ludovice, P. J.; Henderson, C. L. *Thin Solid Films* **2004**, *449* (1−2), 231–241.
(18) Bhattacharya, M.; Sanyal, M. K.; Geue, T.; Pietsch, U. *Phys. Rev. E* **2005**, *71*, 041801.
(19) Fryer, D. S.; Peters, R. D.; Kim, E. J.; Tomaszewski, J. E.; de Pablo, J. J.; Nealey, P. F.; White, C. C.; Wu, W.-l. *Macromolecules* **2001**, *34* (16), 5627–5634.
(20) Kanaya, T.; Miyazaki, T.; Watanabe, H.; Nishida, K.; Yamano, H.; Tasaki, S.; Bucknall, D. B. *Polymer* **2003**, *44* (14), 3769–3773.
(21) Miyazaki, T.; Nishida, K.; Kanaya, T. *Phys. Rev. E* **2004**, *69*, 061803.
(22) Orts, W. J.; van Zanten, J. H.; Wu, W.-l.; Satija, S. K. *Phys. Rev. Lett.* **1993**, *71*, 867.
(23) Pochan, D. J.; Lin, E. K.; Satija, S. K.; Wu, W.-l. *Macromolecules* **2001**, *34* (9), 3041–3045.
(24) Wallace, W. E.; van Zanten, J. H.; Wu, W. L. *Phys. Rev. E* **1995**, *52*, R3329.
(25) Wu, W.-l.; van Zanten, J. H.; Orts, W. J. *Macromolecules* **1995**, *28* (3), 771–774.
(26) Kajiyama, T.; Tanaka, K.; Satomi, N.; Takahara, A. *Macromolecules* **1998**, *31* (15), 5150–5151.
(27) Kajiyama, T.; Tanaka, K.; Takahara, A. *Polymer* **1998**, *39* (19), 4665–4673.
(28) Satomi, N.; Takahara, A.; Kajiyama, T. *Macromolecules* **1999**, *32* (13), 4474–4476.
(29) Forrest, J. A.; Dalnoki-Veress, K.; Dutcher, J. R. *Phys. Rev. E* **1997**, *56*, 5705.
(30) Ata, S.; Muramatsu, M.; Takeda, J.; Ohdaira, T.; Suzuki, R.; Ito, K.; Kobayashi, Y.; Ougizawa, T. *Polymer* **2009**, *50* (14), 3343–3346.
(31) DeMaggio, G. B.; Frieze, W. E.; Gidley, D. W.; Zhu, M.; Hristov, H. A.; Yee, A. F. *Phys. Rev. Lett.* **1997**, *78*, 1524.
(32) Xie, L.; DeMaggio, G. B.; Frieze, W. E.; DeVries, J.; Gidley, D. W.; Hristov, H. A.; Yee, A. F. *Phys. Rev. Lett.* **1995**, *74*, 4947.
(33) Ellison, C. J.; Torkelson, J. M. *Nat. Mater.* **2003**, *2* (10), 695–700.
(34) Kim, S.; Roth, C. B.; Torkelson, J. M. *J. Polym. Sci., Part B: Polym. Phys.* **2008**, *46* (24), 2754–2764.
(35) Priestley, R. D.; Broadbelt, L. J.; Torkelson, J. M.; Fukao, K. *Phys. Rev. E* **2007**, *75* (6), 061806.
(36) Truskett, T. M.; Ganesan, V. *J. Chem. Phys.* **2003**, *119* (4), 1897–1900.
(37) Alcoutlabi, M.; McKenna, G. B. *J. Phys.: Condens. Matter* **2005**, *17* (15), R461.
(38) Baschnagel, J.; Varnik, F. *J. Phys.: Condens. Matter* **2005**, *17* (32), R851.
(39) Ferreira, P. G.; Ajdari, A.; Leibler, L. *Macromolecules* **1998**, *31* (12), 3994–4003.
(40) Ge, S.; Guo, L.; Rafailovich, M. H.; Sokolov, J.; Overney, R. M.; Buenviaje, C.; Peiffer, D. G.; Schwarz, S. A. *Langmuir* **2001**, *17* (5), 1687–1692.
(41) Henn, G.; Bucknall, D. G.; Stamm, M.; Vanhoorne, P.; Jerome, R. *Macromolecules* **1996**, *29* (12), 4305–4313.
(42) Kerle, T.; Yerushalmi-Rozen, R.; Klein, J. *Macromolecules* **1998**, *31* (2), 422–429.
(43) Liu, Y.; Rafailovich, M. H.; Sokolov, J.; Schwarz, S. A.; Bahal, S. *Macromolecules* **1996**, *29* (3), 899–906.
(44) Liu, Y.; Rafailovich, M. H.; Sokolov, J.; Schwarz, S. A.; Zhong, X.; Eisenberg, A.; Kramer, E. J.; Sauer, B. B.; Satija, S. *Phys. Rev. Lett.* **1994**, *73* (3), 440.
(45) Long, D.; Ajdari, A.; Leibler, L. *Langmuir* **1996**, *12* (6), 1675–1680.
(46) Long, D.; Ajdari, A.; Leibler, L. *Langmuir* **1996**, *12* (21), 5221–5230.
(47) Maas, J. H.; Fleer, G. J.; Leermakers, F. A. M.; Cohen Stuart, M. A. *Langmuir* **2002**, *18* (23), 8871–8880.
(48) Maas, J. H.; Leermakers, F. A. M.; Fleer, G. J.; Cohen Stuart, M. A. *Macromol. Symp.* **2003**, *191*, 69.
(49) Matsen, M. W. *J. Chem. Phys.* **2005**, *122* (14), 144904.
(50) Matsen, M. W.; Gardiner, J. M. *J. Chem. Phys.* **2001**, *115* (6), 2794–2804.
(51) Reiter, G.; Auroy, P.; Auvray, L. *Macromolecules* **1996**, *29* (6), 2150–2157.
(52) Reiter, G.; Khanna, R. *Phys. Rev. Lett.* **2000**, *85* (26), 5599.
(53) Reiter, G. S., J.; Auroy, P.; Auvray, L. *Europhys. Lett.* **1996**, *33*, 29.
(54) Shull, K. R. *Faraday Discuss.* **1994**, 98.
(55) Voronov, A.; Shafranska, O. *Langmuir* **2002**, *18* (11), 4471–4477.
(56) Zhang, X.; Lee, F. K.; Tsui, O. K. C. *Macromolecules* **2008**, *41* (21), 8148–8151.
(57) Kim, B.; Ryu, D. Y.; Pryamitsyn, V.; Ganesan, V. *Macromolecules* **2009**, *42* (20), 7919–7923.
(58) Tate, R. S.; Fryer, D. S.; Pasqualini, S.; Montague, M. F.; de Pablo, J. J.; Nealey, P. F. *J. Chem. Phys.* **2001**, *115* (21), 9982–9990.
(59) McCoy, J. D.; Curro, J. G. *J. Chem. Phys.* **2002**, *116* (21), 9154–9157.
(60) Gennes, P. G. d. *Eur. Phys. J. E* **2000**, *2* (3), 201–205.
(61) Ferreira, P. G.; Ajdari, A.; Leibler, L. *Macromolecules* **1998**, *31*, 3994.
(62) Semenov, A. N. *Macromolecules* **1993**, *26* (9), 2273–2281.
(63) Narayanan, B.; Ganesan, V. *Phys. Fluids* **2006**, *18* (4), 042109.
(64) Narayanan, B.; Pryamitsyn, V. A.; Ganesan, V. *Macromolecules* **2004**, *37* (26), 10180–10194.
(65) Pastorino, C.; Binder, K.; Müller, M. *Macromolecules* **2008**, *42* (1), 401–410.
(66) Long, D.; Lequeux, F. *Eur. Phys. J. E* **2001**, *4* (3), 371–387.
(67) Lipson, J., E.G.; Milner, S., T. *Eur. Phys. J. B* **2009**, *72* (1), 133–137.
(68) Kropka, J. M.; Pryamitsyn, V.; Ganesan, V. *Phys. Rev. Lett.* **2008**, *101* (7), 075702.
(69) Pryamitsyn, V.; Ganesan, V. *Macromolecules* **2010**, *43* (13), 5851–5862.